

---

# Uncertainty Calibration for Ensemble-Based Debiasing Methods

---

Ruibin Xiong<sup>1,2,3\*</sup>, Yimeng Chen<sup>2,4\*†</sup>, Liang Pang<sup>2,5</sup>, Xueqi Cheng<sup>1,2</sup>,  
Zhiming Ma<sup>2,4</sup> and Yanyan Lan<sup>6‡</sup>

<sup>1</sup>CAS Key Laboratory of Network Data Science and Technology,  
Institute of Computing Technology, Chinese Academy of Sciences

<sup>2</sup>University of Chinese Academy of Sciences <sup>3</sup>Baidu Inc.

<sup>4</sup>Academy of Mathematics and Systems Science, Chinese Academy of Sciences

<sup>5</sup>Data Intelligence System Research Center,  
Institute of Computing Technology, Chinese Academy of Sciences

<sup>6</sup> Institute for AI Industry Research, Tsinghua University  
{xiongruibin18, chenymeng14}@mailsucas.ac.cn,  
{cxq, pangliang}@ict.ac.cn,  
mazm@amt.ac.cn, lanyanyan@tsinghua.edu.cn

## Abstract

Ensemble-based debiasing methods have been shown effective in mitigating the reliance of classifiers on specific dataset bias, by exploiting the output of a bias-only model to adjust the learning target. In this paper, we focus on the bias-only model in these ensemble-based methods, which plays an important role but has not gained much attention in the existing literature. Theoretically, we prove that the debiasing performance can be damaged by inaccurate uncertainty estimations of the bias-only model. Empirically, we show that existing bias-only models fall short in producing accurate uncertainty estimations. Motivated by these findings, we propose to conduct calibration on the bias-only model, thus achieving a three-stage ensemble-based debiasing framework, including bias modeling, model calibrating, and debiasing. Experimental results on NLI and fact verification tasks show that our proposed three-stage debiasing framework consistently outperforms the traditional two-stage one in out-of-distribution accuracy.

## 1 Introduction

Machine learning models have achieved remarkable performance on natural language understanding [13; 9; 33] and computer vision [19; 20]. However, observations have shown that these models have difficulties in generalizing well in out-of-distribution settings [35; 46; 3; 14], which limits their applications to real-world scenarios. A major cause of this failure is the reliance of the model on specific *dataset bias* [39]. For instance, McCoy et al. [28] have shown that sentence pairs with high word overlaps in MNLI are easy to be classified as the label ‘entailment’, even if they have different relations.

A growing body of literature recognizes debiasing as an important direction in machine learning and natural language processing [44; 4; 5; 40]. Within these works, *ensemble-based debiasing* (EBD) methods [18; 27; 10; 45; 7] have caused considerable interest within the community, as shown

---

\*Equal contribution.

†Work done while Yimeng Chen was interning at Institute for AI Industry Research, Tsinghua University.

‡Corresponding author.

promising improvements on the out-of-distribution performance. EBD methods, e.g., PoE [10], DRiFt [18], and Inverse-Reweight [45], usually adopt a two-stage framework. Firstly, a biased predictor is trained based on the bias features only, namely the *bias-only model*. Its output is then utilized to adjust the learning target of the *main model* by using different ensembling strategies. Previous works are mainly limited to designing different ensembling strategies, without considering the bias-only model, which clearly plays an essential role in the whole process.

In this paper, we focus on investigating the bias-only model in the EBD methods. We theoretically reveal that the quality of the predictive uncertainty estimation given by the bias-only model is crucial for the debiasing performance of EBD methods. Specifically, we prove that the out-of-distribution accuracy of the debiased model is monotonically decreasing with the calibration error of the bias-only model when such error exceeds a threshold<sup>4</sup>. Moreover, by theoretically analyzing the decline of in-distribution performance caused by debiasing, we show the existence of the case when uncertainty calibration can also mitigate such a side-effect. Empirically, we show that bias-only models employed by existing methods on both natural language inference and fact verification tasks fail to produce accurate uncertainty estimations. These findings indicate the critical role of the calibration property of current bias-only models for further improvement of EBD methods.

Motivated by the theoretical analysis and empirical study, we introduce an additional calibration stage into the previous EBD methods. In this stage, the bias-only model is calibrated with model-agnostic calibration methods to obtain more accurate predictive uncertainty estimation. Specifically, two typical calibration methods are used in this paper, i.e. temperature scaling [15] and Dirichlet calibration [24]. After that, the calibrated bias-only model is used to train the main model with off-the-shelf ensembling strategies. In this way, we extend the traditional two-stage EBD framework to a three-stage one, including bias **M**odeling, model **C**alibrating, and **D**ebiasing, named MoCaD for short.

To demonstrate the effectiveness of our proposed framework, we conduct experiments on four challenging benchmarks for two NLU tasks, i.e. natural language inference and fact verification. Experimental results show that our framework significantly improves the out-of-distribution performance, as compared with the traditional two-stage one. Moreover, our theoretical results are well verified by the empirical observations in real scenarios.

Our main contributions can be summarized as the following three folds.

- We explore, both theoretically and empirically, the effect of the bias-only model in the EBD methods. Consequently, a critical problem is revealed: existing bias-only models are poorly calibrated, which will hurt the debiasing performance.
- We propose a model-agnostic three-stage EBD framework to tackle the above problem.
- We conduct extensive experiments on four challenging datasets for two different tasks, and experimental results show the superiority of our proposed framework as against the traditional two-stage one.

## 2 Related Work

**Dataset Bias.** Various biases have been found in different NLU benchmarks. For example, models with partial input can perform much better than majority-class baselines in NLI and fact verification datasets [16; 32; 35]. Many multi-hop questions can be solved by just using single-hop models in the recent multi-hop QA datasets [29; 8]. Similar phenomena have been observed in many other tasks, such as reading comprehension [23] and visual question-answering [1]. Many models have used such superficial cues to achieve remarkable performance instead of capturing the underlying intrinsic principles in these biased datasets, leading to poor generalization on out-of-distribution datasets, when the relation of bias features and labels are changed [28; 35; 26].

**Ensemble-based debiasing (EBD) methods.** EBD methods are a kind of model-agnostic debiasing method to reduce the reliance of models on specific dataset bias. In these methods, a bias-only

---

<sup>4</sup>This condition is more general when the ground truth labeling based on the signal features has low certainty. Such cases exist in natural language understanding (NLU) tasks, where the ground-truth label for a sample is not unique but inherently forms a distribution, as shown by recent empirical studies [31; 30]. That is why we focus our empirical study on NLU tasks.

model is used to assist the debiasing training of the main model. Most EBD methods, e.g., PoE [10], DRiFt [18], and Inverse-Reweight [45], can be formalized as a two-stage framework. It is commonly assumed that the dataset bias is known a-priori. In the first stage, the bias-only model is trained to capture the dataset bias by leveraging the pre-defined bias features. Then the bias-only model is used to adjust the learning target of the main model with different ensembling strategies. Recently, some works start to improve the EBD methods by exploring the bias-only models. For example, Utama et al. [41], Sanh et al. [34], and Clark et al. [11] focus on relaxing the basic assumption of many EBD methods, i.e., the dataset bias is known a-priori. They exploit different prior knowledge to obtain bias-only models, e.g., models that shallow [41] or with limited capacity [34; 11] are considered to be biased. Unlike these works, we theoretically study the essential effect of the bias-only model on the final debiasing performance and show how to improve it in the algorithm design process. Please note that some works [27; 11] have been proposed to jointly learn the bias-only model and the debiased main model in an end-to-end manner. However, Since it is difficult to quantify the impact of the bias-only model in this scheme, we mainly focus on the typical two-stage methods [10; 18; 45; 41; 34].

### 3 Formalization of EBD Methods

In this section, we formalize EBD methods with an introduction to some related notations. Consider a general classification task, where the target is to map an input value  $x \in \mathcal{X}$  of an input random variable  $X$  to a target label  $y \in \mathcal{Y}$  of a target random variable  $Y$ . We denote features of  $x$  that have invariant relations with the label as signal  $x^s$ , e.g., the sentiment words in sentiment analysis. Conversely, features whose correlation with label  $Y$  is spurious and prone to change in the out-of-distribution setting are denoted as bias  $x^b$ , e.g., the length of input sentences in the NLU tasks. The corresponding random variables are respectively denoted as  $X^S$  and  $X^B$ . Now suppose that on a training dataset  $\mathcal{D}$  where  $(X, Y) \sim \mathbb{P}_{\mathcal{D}}(\mathcal{X} \times \mathcal{Y})$ ,  $X^B$  and  $Y$  are spuriously correlated. The goal of debiasing is to learn a classifier that models  $\mathbb{P}_{\mathcal{D}}(Y|X^S)$  with invariant out-of-distribution performance.

The following decomposition forms the theoretical basis for EBD methods: for  $\forall x \in \mathcal{X}$ , with its corresponding features  $X^B = x^b, X^S = x^s$ ,

$$\mathbb{P}_{\mathcal{D}}(Y|X = x) \propto \mathbb{P}_{\mathcal{D}}(Y|X^B = x^b)\mathbb{P}_{\mathcal{D}}(Y|X^S = x^s)\frac{1}{\mathbb{P}_{\mathcal{D}}(Y)}, \quad (1)$$

where  $\mathbb{P}_{\mathcal{D}}(Y|X^B = x^b)$  is the conditional probability distribution of  $Y$  given the value of bias features  $X^B$ ,  $\mathbb{P}_{\mathcal{D}}(Y|X^S = x^s)$  represents the true principle we would like to learn, and  $\mathbb{P}_{\mathcal{D}}(Y|X = x)$  is the conditional distribution of  $Y$  given all features, which is usually approximated by directly applying statistical machine learning methods on the training data. This decomposition can be deduced under the constraint that  $X^S \perp\!\!\!\perp X^B|Y$ , as shown in [10; 18; 11]. We further prove that it also holds with the assumptions in [45] (See the appendix). The theoretical analysis in this paper is conducted based on the same constraint as in [10; 18; 11].

From this decomposition, the true principle  $\mathbb{P}_{\mathcal{D}}(Y|X^S)$  can be achieved by adjusting the learning target with  $\mathbb{P}_{\mathcal{D}}(Y|X^B)$ . This is exactly the basic idea of EBD methods.

Most EBD methods belong to a two-stage framework. In the first stage, a bias-only model  $f_B : \mathcal{X} \rightarrow \mathbb{R}^{|\mathcal{Y}|}$  is trained to approximate  $\mathbb{P}_{\mathcal{D}}(Y|X^B)$ . Then it is employed to adjust the learning target in a direct or indirect way. Direct methods such as Inverse-Reweight [45] reweight the distribution by the inverse of the probability induced by the bias-only model to approximate the true principle. The objective function of the main model  $f_M : \mathcal{X} \rightarrow \mathbb{R}^{|\mathcal{Y}|}$  becomes:

$$\min_{f_M} \mathbb{E}_{X, Y \sim \mathbb{P}_{\mathcal{D}}} \left[ \frac{1}{p_Y^b(X)} \mathcal{L}_c(Y, \mathbf{p}^m(X)) \right], \quad (2)$$

where  $\mathbf{p}^b(X) = \{p_1^b(X), p_2^b(X), \dots, p_{|\mathcal{Y}|}^b(X)\}$ ,  $\mathbf{p}^m(X) = \{p_1^m(X), p_2^m(X), \dots, p_{|\mathcal{Y}|}^m(X)\}$  denote the uncertainty estimations, i.e. the prediction probabilities given by  $f_B$  and  $f_M$  respectively.  $\mathcal{L}_c$  represents the cross-entropy loss function. On the other hand, indirect methods usually utilize the output of the bias-only model to adjust the loss function of the main model, and the learning target becomes:

$$\min_{f_M} \mathbb{E}_{X, Y \sim \mathbb{P}_{\mathcal{D}}} [\mathcal{L}_c(Y, m(\mathbf{q}^b(X) \cdot \mathbf{q}^m(X)))] \quad (3)$$

where  $m$  is the normalization function, and  $\mathbf{q}^b(X)$ ,  $\mathbf{q}^m(X)$  are vectors in proportion to  $\mathbf{p}^b(X)$  and  $\mathbf{p}^m(X)$  respectively. Specifically, PoE [10; 41] directly uses the probability output, DRiFt [18] and Sanh et al. [34] utilizes exponential of the logits output. In Learned-Mixin [10], a variant of PoE,  $\mathbf{q}^b(X)$  is changed to  $(\mathbf{p}^b(X))^{g(X)}$ , where  $g(X)$  is a trainable gate function.

For both direct and indirect methods, by the property of the cross-entropy loss [17], the optimal main model  $f_M^*$  satisfies  $\mathbf{p}^{m*} \propto \mathbb{P}_{\mathcal{D}}(Y|X)/\mathbf{p}^b$ . Therefore, we have  $\mathbf{p}^{m*} \propto \mathbb{P}_{\mathcal{D}}(Y|X^S)$  when  $\mathbf{p}^b \propto \mathbb{P}_{\mathcal{D}}(Y|X^B)$ , which guarantees the effectiveness of the existing EBD methods. Please note that Learned-Mixin does not satisfy this property due to the trainable gate function.

## 4 Analysis of the Bias-only Model

Bias-only models are critical to EBD methods, since their outputs are used to help recover the unbiased distribution. However, far too little attention has been paid to them in previous research. In this section, we theoretically quantify the effect of bias-only outputs on the final debiasing performance and empirically show the weakness of existing bias-only models.

### 4.1 Theoretical Analysis

According to the discussion in Section 3, the optimal main model  $f_M^*$  induces the following conditional probability:

$$\mathbb{P}_{\mathcal{D}, f_M^*}(Y = i|X) := \frac{\mathbb{P}_{\mathcal{D}}(Y = i|X)/p_i^b(X)}{\sum_{j \in \mathcal{Y}} \mathbb{P}_{\mathcal{D}}(Y = j|X)/p_j^b(X)}. \quad (4)$$

For arbitrary  $x \in \mathcal{X}$ , we define

$$Y(x) := \operatorname{argmax}_{i \in \mathcal{Y}} \mathbb{P}_{\mathcal{D}}(Y = i|X^S = x^s), \tilde{Y}(x) := \operatorname{argmax}_{i \in \mathcal{Y}} \mathbb{P}_{\mathcal{D}, f_M^*}(Y = i|X = x). \quad (5)$$

Here  $Y(x)$  stands for the predicted label given by the intrinsic principle, and  $\tilde{Y}(x)$  is the label prediction given by the debiased main model. With these notations, the debiasing performance can be defined as  $\mathbb{E}_{X \sim \mathbb{P}_{\mathcal{D}}(X)}(\tilde{Y}(X) = Y(X))$ . As the major factor related to the bias-only model is  $p_i^b(X)$ , i.e. the uncertainty estimation, in the concerned quantities  $\tilde{Y}(X)$ , we investigate the effect of the bias-only model on the debiasing performance from this aspect.

Without loss of generality, we consider the binary classification problem with  $\mathcal{Y} = \{0, 1\}$  and balanced label distribution. To divide and conquer, we conduct the theoretical analysis on a set of samples, where the bias-only model generates the same uncertainty estimation, i.e.  $\mathcal{S}_{f_B}(l) := \{x | p_0^b(x) = l\}, \forall l \in [0, 1]$ . Specifically, the quality of the uncertainty estimation of the bias-only model on  $\mathcal{S}_{f_B}(l)$  can be measured by the calibration error defined as  $|l - \mathbb{P}_{\mathcal{D}}(Y = 0|\mathcal{S}_{f_B}(l))|$ . The debiasing performance on  $\mathcal{S}_{f_B}(l)$  is defined as  $\mathbb{P}_{\mathcal{D}}(\{x \in \mathcal{S}_{f_B}(l) | \tilde{Y}(x) = Y(x)\})$ , i.e. the probability of the subset of  $\mathcal{S}_{f_B}(l)$  on which the main model gives the same prediction as the intrinsic principle.

The following theorem formalizes a precise result. Specifically, the debiasing performance is a monotonically decreasing function of the calibration error when it exceeds a deviation threshold  $\delta(l_0, \epsilon, \alpha)$ . Here  $\alpha := \min_{X^S} \max_{i \in \{0, 1\}} \mathbb{P}_{\mathcal{D}}(Y = i|X^S)$  denotes the global certainty level of the true principle  $\mathbb{P}_{\mathcal{D}}(Y|X^S)$ .

**Theorem 1.** *For any  $l \in [0, 1]$ , assume that  $\exists l_0$  s.t.  $\mathbb{P}_{\mathcal{D}}(Y = 0|X^B) \in (l_0 - \epsilon, l_0 + \epsilon)$  when  $X$  takes values in  $\mathcal{S}_{f_B}(l)$ . If the calibration error  $|l - \mathbb{P}_{\mathcal{D}}(Y = 0|\mathcal{S}_{f_B}(l))| \geq \delta(l_0, \epsilon, \alpha) > 0$ , the debiasing performance  $\mathbb{P}_{\mathcal{D}}(\{x \in \mathcal{S}_{f_B}(l) | \tilde{Y}(x) = Y(x)\})$  declines as  $|l - \mathbb{P}_{\mathcal{D}}(Y = 0|\mathcal{S}_{f_B}(l))|$  increases, where  $\delta(l_0, \epsilon, \alpha)$  is a constant dependent with  $l_0, \epsilon$  and  $\alpha$ . When  $\alpha < \frac{1}{2} + \frac{\epsilon}{2l_0(1-l_0)+2\epsilon^2}$ ,  $0 \leq \delta(l_0, \epsilon, \alpha) < 2\epsilon$ , where  $2\epsilon \leq \frac{\epsilon}{2l_0(1-l_0)+2\epsilon^2} < \frac{1}{2}$ . Otherwise  $C < \delta(l_0, \epsilon, \alpha) < 2\epsilon + C$ , where  $0 < C := l_0 - \epsilon - \frac{l_0 + \epsilon}{(l_0 + \epsilon) + (1 - l_0 - \epsilon)\frac{\alpha}{1-\alpha}}$ , which increases as  $\alpha$  increases.*

The threshold in this theorem depends on latent constants  $l_0, \epsilon$ , and  $\alpha$ . Here  $l_0$  and  $\epsilon$  define the range of  $\mathbb{P}_{\mathcal{D}}(Y = 0|X^B)$  on  $\mathcal{S}_{f_B}(l)$ . As these constants are related to the posterior characteristics of  $f_B$ , we verify the generality of such condition by empirical facts in Section 6. Note that the deviation threshold decreases as the certainty level  $\alpha$  decreases. That means the same calibration error is more likely to exceed the threshold under smaller  $\alpha$ , resulting in a more considerable decrease in debiasing

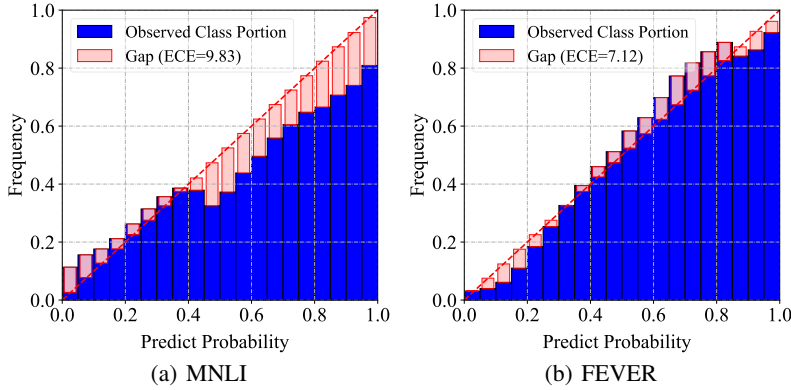


Figure 1: Reliability diagrams of the bias-only models on MNL and FEVER. The x-axis is the predictive probability of the bias-only model, and the y-axis is the frequency. The wide blue bars show the weighted average of the observed class portion to all classes within each bin, and the narrow red bars show the gap between the observed class portion and the predictive probability of the bias-only model.

performance. As a result, the condition in Theorem 1 is more general and significant when the true principle  $\mathbb{P}_{\mathcal{D}}(Y|X^S)$  has low certainty, for example, in the NLU tasks as supported by empirical evidence in [31; 30].

We also theoretically analyze the effect of the bias-only model on the in-distribution performance, which is defined as  $\mathbb{E}_{X \sim \mathbb{P}_{\mathcal{D}}(X)}(\tilde{Y}(X) = \hat{Y}(X))$ , where  $\hat{Y}(x) := \operatorname{argmax}_{i \in \mathcal{Y}} \mathbb{P}_{\mathcal{D}}(Y = i|X = x)$  denotes the label given by the ideal predictor on  $\mathcal{D}$ . The result is shown in the following theorem.

**Theorem 2.** *For any  $X$ ,  $\tilde{Y}(X) \neq \hat{Y}(X)$  if and only if  $p_{\hat{Y}(x)}^b(x) > \mathbb{P}_{\mathcal{D}}(Y = \hat{Y}(x)|X = x)$ .*

Theorem 2 gives a possible explanation for the decrease of in-distribution performance of EBD debiased models: the in-distribution error occurs when the predictive uncertainty estimation of the bias-only model on  $\hat{Y}(x)$  is higher than the conditional probability of  $\hat{Y}(x)$ . That indicates that the in-distribution error is non-decreasing as the range of the uncertainty estimation of bias-only models increases. As an important case, when the bias-only model is over-confident [15], decreasing its calibration error can improve both the in-distribution and out-of-distribution performance of the debiased model according to the two theorems.

To sum up, our theoretical study shows that both debiasing and in-distribution performances of the EBD methods are affected by the uncertainty estimation of the bias-only models. Please note that both Theorem 1 and 2 can be generalized to multi-class scenarios, with a more complex form. For simplicity, we only discuss the binary class case.

## 4.2 Empirical Analysis

According to some recent machine learning studies, the uncertainty estimations of many widely used machine learning classifiers are not reliable [25; 15; 38; 42]. This indicates that the existing bias-only classifiers may fail to produce a good uncertainty estimation, which can hurt the debiasing performance, as demonstrated by our theoretical results.

To quantify the effect, we further conduct an empirical study to demonstrate the quality of the existing bias-only models with respect to the uncertainty estimation. Specifically, we experiment on two typical public datasets, MNL and FEVER. Their experimental settings and detailed analysis can be found in Section 6.1. For MNL, we consider the syntactic bias [28] and use hand-crafted features to train a bias-only model, the same as in [10]. For FEVER, we consider the claim-only bias [35] and train a claim-only model as the bias-only model, as in [40]. After that, we use the classwise reliability diagram [24] to check its calibration error based on data binning. We adopt the classwise expected calibration error [24] as a measure to quantify the quality of the uncertainty estimation, denoted as ECE for short, with its lower value indicates better-calibrated uncertainty estimation.

Now we introduce our experimental results. The classwise reliability diagrams on MNLi and FEVER training sets are plotted in Figure 1(a) and Figure 1(b), respectively. For perfectly calibrated predictions, the curve in a reliability diagram should be as close as possible to the diagonal. Therefore, the deviation from the diagonal represents the calibration error. From the results, we can see that existing bias-only models suffer from inaccurate uncertainty estimation problems on both datasets.

## 5 The MoCaD Framework

To overcome the unreliable predictive uncertainty problem, we introduce a calibration operation to the bias-only model, achieving a **M**odeling, **C**alibrating and **D**ebiasing framework, named MoCaD for short. Our framework consists of three stages. Firstly, we train a bias-only model to model  $\mathbb{P}_{\mathcal{D}}(Y|X^B)$ . Secondly, we use the model-agnostic calibration methods to improve the calibration error of the bias-only model. The calibrated bias-only model is finally employed to conduct the debiasing process through the existing ensembling strategies.

### 5.1 Bias Modeling

In the first stage, we train a bias-only model to approximate  $\mathbb{P}_{\mathcal{D}}(Y|X^B)$ , similar to previous works [10; 18]. When the dataset bias is identified, i.e. bias features  $X_B$  are known a-priori [10; 18], the bias-only model can be obtained by only using the pre-defined  $X_B$  to predict label  $y$  with cross-entropy loss. For example, in NLI, many specific linguistic phenomena in hypothesis sentences such as negation are highly correlated with certain inference classes [32]. In this case, hypothesis sentences are used as inputs to train an NLI model as a bias-only model. When the dataset bias is unknown, a ‘shallow’ model or a ‘weak’ model can be built as the bias-only model, as in [41; 34].

### 5.2 Model Calibrating

We propose to utilize model-agnostic calibration methods to improve the calibration error of the bias-only models. Specifically, two typical calibration methods, temperature scaling [15] and Dirichlet calibrator [24], are used in this paper. The calibrated bias-only model is denoted as  $\tilde{f}_B$ .

Temperature scaling is a simple-but-effective calibration method. It learns a single scalar parameter ‘temperature’ which is applied to the last softmax layer. Specifically, denote  $\mathbf{z}^b(X)$  as the logit output of the bias-only model on sample  $(X, Y)$ , abbreviated for  $\mathbf{z}^b$ , temperature scaling will correct the output as follows:  $\tilde{\mathbf{p}}^b = \text{softmax}(\mathbf{z}^b/T)$ , where  $T$  is the temperature, which is learned with the cross-entropy loss.

Dirichlet calibrator is derived from the Dirichlet distribution likelihood. The transformed probability is computed as  $\tilde{\mathbf{p}}^b = \text{softmax}(\mathbf{W} \ln \mathbf{p}^b + \mathbf{b}')$ , where  $\mathbf{W}$  and  $\mathbf{b}'$  stand for the linear transformation matrix and intercept term, which are optimized by the cross-entropy loss equipped with ODIR (Off-Diagonal and Intercept Regularisation) to prevent over-fitting [24].

Please note that temperature scaling does not change the predicted label because the maximum of the softmax function remains unchanged. In other words, it only changes the uncertainty estimation and maintains the model’s accuracy. Unlike temperature scaling, the Dirichlet calibrator can change the prediction accuracy. Empirically, we observed that the Dirichlet calibrator improves the accuracy of all bias-only models in our experiments (See the Appendix for details). In both methods, the calibration error is expected to be reduced by learning the parameters with the cross-entropy loss.

### 5.3 Debiasing

The final step is to train the main model  $f_D$  with the calibrated bias-only model  $\tilde{f}_B$ . Specifically,  $\tilde{f}_B$  is applied with the existing ensembling strategies to make the main model  $f_D$  approximate the true principle  $\mathbb{P}_{\mathcal{D}}(Y|X^S)$ , by adjusting the learning target of the main model, as described in Section 3. The design of the main model is highly dependent on the concerned task, as indicated by previous works. For example, a BERT-based classifier is usually used in NLI [18], and a BottomUp-TopDown VQA model is usually adopted in VQA [10].

## 6 Experiments

In this section, we conduct experiments on different real-world datasets to answer two questions: (1) whether our proposed MoCaD framework improves the debiasing performance of the EBD methods; (2) whether the experimental results are consistent with the theoretical findings.

### 6.1 Experimental Settings

We describe our experimental settings, including datasets, models and some training details. More details are provided in the Appendix.

**Datasets and bias-only models.** We conduct experiments on both fact verification and natural language inference, which are commonly used tasks in debiasing [10; 40; 41]. We follow these works to choose the datasets and design the bias-only models.

Fact verification requires models to validate a claim in the context of evidence. For this task, we use the training dataset provided by the FEVER challenge [37]. The processing and split of the dataset into training/development set are conducted following Schuster et al. [35]<sup>5</sup>. It has been shown that FEVER has the claim-only bias, where claim sentences often contain words highly indicative of the target label [35]. So the bias-only model is trained to predict labels by only using claim sentences. Finally, Fever-Symmetric datasets [35] (both version 1 and 2) are used as the test sets for evaluation.

Natural language inference aims to infer the relationship between premise and hypothesis. Recent studies have shown that various biases exist in the widely used NLI datasets [32; 16; 28]. In this paper, we conduct our experiments on MNLI [43] and consider both known bias and unknown bias. For known bias, firstly, we consider the syntactic bias, e.g. the lexical overlap between premise and hypothesis sentences is strongly correlated with the entailment label [28]. So the bias-only model is a classifier using hand-crafted features indicating how words are shared between the two sentences as the input, the same as that in [10]. Finally, HANS (Heuristic Analysis for NLI Systems) [28] is utilized as the challenging dataset for evaluation. Then we consider the hypothesis-only bias, which means that we can only use the hypothesis to predict the relation between premise and hypothesis. So the bias-only model is defined as a classifier trained to predict labels by only using hypothesis. In the experiment, we still use MNLI as the training set and employ two hard MNLI datasets [16; 26] for evaluation. The ‘hard’ subsets are derived from the MNLI Mismatched dataset with two different strategies: (1) a neural classifier is trained on hypothesis sentences and the wrongly classified instances are treated as ‘hard’ instances. (2) patterns in hypothesis sentences that are highly correlated to the specific labels are extracted as surface patterns, and samples which against those surface patterns’ indications are recognized as ‘hard’ samples. Therefore, the two challenging dataset are referred to as Hard-CD (Classifier Detected) and Hard-SP (Surface Pattern), corresponding to their creation strategies. For unknown bias, following Utama et al. [41], we build a ‘shallow’ model as the bias-only model, which has the same architecture as the main model and is trained on a subset of the MNLI training set. Then we use HANS as the challenging dataset for evaluation as Utama et al. [41].

**Baselines and configurations.** We experiment with 8 implementations of MoCaD, i.e. two different calibrators combined with four different ensembling strategies. The two calibrators are temperature scaling and Dirichlet calibrator, and the four ensembling strategies are those in Product-of-Experts (PoE), Learned-Mixin (LMin), DRiFt, and Inverse-Reweight (Inv-R). We compare the performances of these implementations with their corresponding two-stage EBD methods. We denote different implementations of MoCaD by the name of corresponding EBD methods with the calibrator name as the subscript. We use `TempS` and `Dirichlet` to denote the implemented methods with temperature scaling and Dirichlet as the calibrator, respectively.

In our experiments, we adopt the BERT-based classifier as the main model and follow the standard setup for sentence pair classification [13]. The cross-entropy trained model (denoted as CE) is also included as a baseline, to show the difference between the debiased and un-debiased model. To tackle the high performance variance on challenging datasets as observed by Clark et al. [10], we run each experiment five times and report the mean scores and the standard deviations. For each task, we utilize the training configurations that have been proven to work well in previous studies and keep the same bias-only model for all methods. For Learned-Mixin, the entropy term weight is set to the value

<sup>5</sup><https://github.com/TalSchuster/FeverSymmetric>

Table 2: Classification accuracy on MNLI.

Method	Syntactic Bias		Hypothesis-only Bias			Unknown Bias	
	ID	HANS	ID	Hard <sub>CD</sub>	Hard <sub>SP</sub>	ID	HANS
CE	84.2 ± 0.2	61.2 ± 3.2	84.2 ± 0.2	76.8 ± 0.4	72.6 ± 2.0	84.2 ± 0.2	61.2 ± 3.2
PoE	82.8 ± 0.4	68.1 ± 3.4	83.2 ± 0.2	79.4 ± 0.4	76.8 ± 2.4	80.7 ± 0.2	69.0 ± 2.4
<b>PoE</b> <sub>TempS</sub>	83.9 ± 0.3	69.1 ± 2.8	82.9 ± 0.3	79.6 ± 0.4	77.4 ± 2.4	82.1 ± 0.2	69.9 ± 1.6
<b>PoE</b> <sub>Dirichlet</sub>	84.1 ± 0.3	<b>70.7</b> ± 1.5	82.7 ± 0.4	79.4 ± 0.2	<b>77.6</b> ± 2.1	82.3 ± 0.3	<b>70.7</b> ± 1.0
DRiFt	81.8 ± 0.4	66.5 ± 4.0	83.5 ± 0.4	79.5 ± 0.6	76.3 ± 1.6	80.2 ± 0.3	69.1 ± 1.3
<b>DRiFt</b> <sub>TempS</sub>	83.0 ± 0.4	69.7 ± 1.8	83.1 ± 0.2	79.6 ± 0.2	77.4 ± 3.3	81.5 ± 0.3	<b>70.0</b> ± 0.9
<b>DRiFt</b> <sub>Dirichlet</sub>	83.6 ± 0.3	<b>69.8</b> ± 1.9	82.8 ± 0.3	79.6 ± 0.2	<b>79.0</b> ± 1.6	81.9 ± 0.6	69.4 ± 1.1
InvR	82.5 ± 0.1	68.4 ± 1.2	83.1 ± 0.2	78.4 ± 0.5	77.1 ± 2.0	78.7 ± 4.8	64.7 ± 2.6
<b>InvR</b> <sub>TempS</sub>	83.6 ± 0.2	69.4 ± 1.6	82.8 ± 0.2	78.6 ± 0.2	77.9 ± 1.7	81.4 ± 0.5	65.8 ± 0.9
<b>InvR</b> <sub>Dirichlet</sub>	83.7 ± 0.4	<b>69.4</b> ± 1.3	82.5 ± 0.2	78.9 ± 0.4	<b>80.8</b> ± 2.0	81.5 ± 0.2	<b>68.2</b> ± 0.8
LMin	84.1 ± 0.3	<b>65.5</b> ± 3.7	80.5 ± 0.3	80.0 ± 0.4	78.2 ± 2.0	83.1 ± 0.3	<b>66.5</b> ± 1.1
<b>LMin</b> <sub>TempS</sub>	84.1 ± 0.2	63.2 ± 2.7	80.5 ± 0.6	80.3 ± 0.2	80.8 ± 3.6	83.3 ± 0.2	66.2 ± 1.0
<b>LMin</b> <sub>Dirichlet</sub>	84.3 ± 0.3	62.7 ± 2.6	80.1 ± 0.5	79.8 ± 0.4	<b>83.2</b> ± 2.2	82.7 ± 0.2	66.4 ± 1.2

suggested by Utama et al. [40]. For the Dirichlet calibrator, we set  $\lambda = 0.06$  for all experiments, based on the in-distribution performance on the development sets.

## 6.2 Experimental Results

Now we show our experimental results to answer the aforementioned two questions.

Table 1 shows the experimental results on FEVER. We can see that for both calibrators, MoCaD outperforms the corresponding EBD methods, including Learned-Mixin, on both Fever-Symmetric v1 and v2 datasets. Comparing different calibrators, `Dirichlet` consistently performs better than `TempS`. Please note that the label distribution of the development set is different from that of the training set on FEVER, which explains why sometimes `Dirichlet` obtains better in-distribution performance than the cross-entropy loss.

Table 2 shows the experimental results on MNLI with respect to known bias and unknown bias. The main results are similar to that on FEVER, i.e. calibration brings benefit to the debiasing performance, and `Dirichlet` obtains better results than `TempS`, for all EBD methods except `Learnd-Mixin` on HANS. It indicates that for both known and unknown dataset bias, MoCaD outperforms corresponding EBD methods. Please note that, as a trainable gate function is added in `Learned-Mixin`, the optimal bias-only model of it is different from others and does not fit our theoretical assumptions. Specially, the performance gap between baselines and our methods is relatively small on Hard-CD. This may due to the fact that the construction of Hard-CD is dependent on a specific biased model.

Table 1: Classification accuracy on FEVER.

Method	ID	Symm. v1	Symm. v2
CE	87.1 ± 0.6	56.5 ± 0.9	63.9 ± 0.9
PoE	84.0 ± 1.0	62.0 ± 1.3	65.9 ± 0.6
<b>PoE</b> <sub>TempS</sub>	82.0 ± 0.9	63.3 ± 0.9	66.4 ± 0.8
<b>PoE</b> <sub>Dirichlet</sub>	87.1 ± 1.0	<b>65.9</b> ± 1.1	<b>69.1</b> ± 0.8
DRiFt	84.2 ± 1.2	62.3 ± 1.5	65.9 ± 0.7
<b>DRiFt</b> <sub>TempS</sub>	81.7 ± 0.9	63.5 ± 1.3	66.5 ± 0.7
<b>DRiFt</b> <sub>Dirichlet</sub>	87.4 ± 1.2	<b>65.7</b> ± 1.4	<b>69.0</b> ± 1.3
InvR	84.3 ± 0.8	60.8 ± 1.2	65.2 ± 1.0
<b>InvR</b> <sub>TempS</sub>	83.8 ± 0.6	61.5 ± 0.9	65.4 ± 0.7
<b>InvR</b> <sub>Dirichlet</sub>	87.0 ± 0.8	<b>63.8</b> ± 2.2	<b>68.2</b> ± 1.7
LMin	84.7 ± 1.8	59.8 ± 2.7	65.3 ± 1.1
<b>LMin</b> <sub>TempS</sub>	84.9 ± 1.7	60.0 ± 2.5	65.6 ± 1.5
<b>LMin</b> <sub>Dirichlet</sub>	87.5 ± 1.1	<b>61.5</b> ± 2.4	<b>67.1</b> ± 1.3

### 6.2.1 Empirical Verification of Theorem 1

Now we analyze whether the improvement of debiasing performance agrees with our theoretical study in Theorem 1. That is, calibrated models achieve better uncertainty estimation, leading to better debiasing performance results.



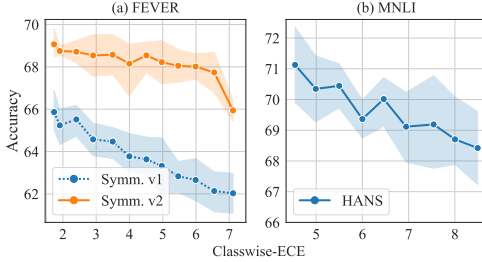


Figure 2: Debiasing performance of bias-only model vs the quality of predictive uncertainty measured by classwise-ECE (lower is better).

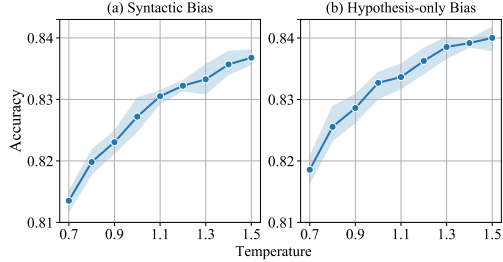


Figure 3: In-distribution performance (accuracy) of the main model vs temperature.

To facilitate the study, we demonstrate the classwise-ECE of the calibrated bias-only models on different training datasets, as shown in Table 3. In the table, Un-Cal, Dirichlet, and TempS denote the bias-only model without calibration, with temperature scaling and Dirichlet calibrator, respectively. From the results, we can see that calibrated bias-only models on different datasets achieve better uncertainty estimation, for both calibrators. Comparing the two calibrators, the Dirichlet calibrator performs better because of its higher expressive power. Further considering the debiasing improvement in Table 1 and 2, we can see that the empirical findings consist with our theory.

Furthermore, we conduct a more detailed experiment on MNL and FEVER, regarding syntactic bias and claim-only bias respectively. Specifically, we adopt the ensembling strategy in PoE, and calibrate bias-only models with the Dirichlet calibrator and save models at different checkpoints. Then we consider the debiasing performances of bias-only models with different uncertainty estimation qualities, measured by classwise-ECE. The results are plotted in Figure 2. We can see that when the classwise-ECE grows, i.e. the calibration error of the bias-only model grows, the accuracy on the test set decreases, i.e. the debiasing performance drops. These results precisely prove Theorem 1.

### 6.2.2 Empirical Verification of Theorem 2

Theorem 2 reveals the relation between the confidence of the bias-only model and the in-distribution error of the main model. That is, if the confidence, i.e. the uncertainty estimation of the bias-only model on the predicted label is reduced, the in-distribution error of the main model will decrease. Since the label distribution changes on the development set of FEVER, we only consider the results on MNL. From Table 2, the in-distribution performance increases in the scenario of syntactic and unknown bias and decreases in the scenario of hypothesis-only bias, for most implementations. That is because the syntactic and unknown bias-only model is over-confident, and the hypothesis-only bias-only model is under-confident, as shown in our Appendix. These results are accordant with our theory.

We provide a detailed experiment to further explain the relationship revealed in Theorem 2. Specially, we adopt the ensembling strategy in PoE and take temperature scaling as the calibrator, because the temperature parameter controls the confidence of the calibrated model. The bigger the temperature, the less confident the obtained model. We manually set the temperature parameter from 0.7 to 1.5 with step 0.1, and record the in-distribution accuracy on the development set for the calibrated bias-only model with PoE. The results are plotted in Figure 3. It shows that when the bias-only model is less confident, the in-distribution performance of the main model improves, which verifies Theorem 2.

We provide a detailed experiment to further explain the relationship revealed in Theorem 2. Specially, we adopt the ensembling strategy in PoE and take temperature scaling as the calibrator, because the temperature parameter controls the confidence of the calibrated model. The bigger the temperature, the less confident the obtained model. We manually set the temperature parameter from 0.7 to 1.5 with step 0.1, and record the in-distribution accuracy on the development set for the calibrated bias-only model with PoE. The results are plotted in Figure 3. It shows that when the bias-only model is less confident, the in-distribution performance of the main model improves, which verifies Theorem 2.

## 7 Conclusions and Future Work

This paper theoretically and empirically reveals an important problem, which is ignored in previous studies, that existing bias-only models in the EBD methods are poor-calibrated, leading to unsatis-

Table 3: Classwise-ECE of the calibrated bias-only models on different training datasets.

	FEVER	HANS	MNL	Unknown
Un-Cal	7.11	9.83	3.01	7.41
TempS	6.23	7.70	2.38	3.07
Dirichlet	1.73	4.47	0.87	1.45

factory debiasing performances. To tackle this problem, we propose a three-stage EBD framework (MoCaD), including bias modeling, model calibrating, and debiasing. Extensive experiments on natural language inference and fact verification tasks show that MoCaD outperforms corresponding EBD methods, regarding known and unknown dataset bias. Furthermore, our detailed empirical analyses verify the correctness of our theorems. We believe that our study will draw people’s attention to the bias-only model, which has the potential to become an interesting research direction in the debiasing study. A limitation of this paper is that our empirical studies focus on NLU tasks. Further experimental results on image classification show inconsistent improvements (See the appendix). A possible reason is that image classes (e.g., birds or elephants) are less disputed than language concepts (e.g., entailment or neutral). Thus the invariant mechanism for image classification has a higher certainty, reducing the impact of calibration error on debiasing according to our theoretical analysis. In the future, we plan to extend our investigations to end-to-end EBD methods and more tasks besides NLU.

## Acknowledgments and Disclosure of Funding

This work is supported by the National Key R&D Program of China under Grants No. 2020AAA0105200, the National Natural Science Foundation of China (NSFC) under Grants No. 61773362, and 61906180.

## References

- [1] Aishwarya Agrawal, Dhruv Batra, and Devi Parikh. Analyzing the behavior of visual question answering models. In *Proceedings of the 2016 Conference on Empirical Methods in Natural Language Processing*, pages 1955–1960, 2016.
- [2] Hyojin Bahng, Sanghyuk Chun, Sangdoon Yun, Jaegul Choo, and Seong Joon Oh. Learning de-biased representations with biased representations. In *International Conference on Machine Learning*, pages 528–539. PMLR, 2020.
- [3] Sara Beery, Grant Van Horn, and Pietro Perona. Recognition in terra incognita. In *Proceedings of the European Conference on Computer Vision (ECCV)*, pages 456–473, 2018.
- [4] Yonatan Belinkov, Adam Poliak, Stuart M Shieber, Benjamin Van Durme, and Alexander Rush. On adversarial removal of hypothesis-only bias in natural language inference. *NAACL HLT 2019*, page 256, 2019.
- [5] Emily M. Bender and Alexander Koller. Climbing towards NLU: On meaning, form, and understanding in the age of data. In *Proceedings of the 58th Annual Meeting of the Association for Computational Linguistics*, pages 5185–5198, Online, July 2020. Association for Computational Linguistics. doi: 10.18653/v1/2020.acl-main.463. URL <https://www.aclweb.org/anthology/2020.acl-main.463>.
- [6] Wieland Brendel and Matthias Bethge. Approximating cnns with bag-of-local-features models works surprisingly well on imagenet. *arXiv preprint arXiv:1904.00760*, 2019.
- [7] Remi Cadene, Corentin Dancette, Matthieu Cord, Devi Parikh, et al. Rubi: Reducing unimodal biases for visual question answering. In *Advances in neural information processing systems*, pages 841–852, 2019.
- [8] Jifan Chen and Greg Durrett. Understanding dataset design choices for multi-hop reasoning. In *Proceedings of the 2019 Conference of the North American Chapter of the Association for Computational Linguistics: Human Language Technologies, Volume 1 (Long and Short Papers)*, pages 4026–4032, 2019.
- [9] Qian Chen, Xiaodan Zhu, Zhen-Hua Ling, Si Wei, Hui Jiang, and Diana Inkpen. Enhanced lstm for natural language inference. In *Proceedings of the 55th Annual Meeting of the Association for Computational Linguistics (Volume 1: Long Papers)*, pages 1657–1668, 2017.

- [10] Christopher Clark, Mark Yatskar, and Luke Zettlemoyer. Don't take the easy way out: Ensemble based methods for avoiding known dataset biases. In *Proceedings of the 2019 Conference on Empirical Methods in Natural Language Processing and the 9th International Joint Conference on Natural Language Processing (EMNLP-IJCNLP)*, pages 4060–4073, 2019.
- [11] Christopher Clark, Mark Yatskar, and Luke Zettlemoyer. Learning to model and ignore dataset bias with mixed capacity ensembles. In *Proceedings of the 2020 Conference on Empirical Methods in Natural Language Processing: Findings*, pages 3031–3045, 2020.
- [12] Jia Deng, Wei Dong, Richard Socher, Li-Jia Li, Kai Li, and Li Fei-Fei. Imagenet: A large-scale hierarchical image database. In *2009 IEEE conference on computer vision and pattern recognition*, pages 248–255. Ieee, 2009.
- [13] Jacob Devlin, Ming-Wei Chang, Kenton Lee, and Kristina Toutanova. Bert: Pre-training of deep bidirectional transformers for language understanding. In *Proceedings of the 2019 Conference of the North American Chapter of the Association for Computational Linguistics: Human Language Technologies, Volume 1 (Long and Short Papers)*, pages 4171–4186, 2019.
- [14] Robert Geirhos, Patricia Rubisch, Claudio Michaelis, Matthias Bethge, Felix A Wichmann, and Wieland Brendel. Imagenet-trained cnns are biased towards texture; increasing shape bias improves accuracy and robustness. In *ICLR*, 2019.
- [15] Chuan Guo, Geoff Pleiss, Yu Sun, and Kilian Q Weinberger. On calibration of modern neural networks. *arXiv preprint arXiv:1706.04599*, 2017.
- [16] Suchin Gururangan, Swabha Swayamdipta, Omer Levy, Roy Schwartz, Samuel Bowman, and Noah A Smith. Annotation artifacts in natural language inference data. In *Proceedings of the 2018 Conference of the North American Chapter of the Association for Computational Linguistics: Human Language Technologies, Volume 2 (Short Papers)*, pages 107–112, 2018.
- [17] T. Hastie, R. Tibshirani, and J.H. Friedman. *The Elements of Statistical Learning: Data Mining, Inference, and Prediction*. Springer series in statistics. Springer, 2009. ISBN 9780387848846. URL <https://books.google.com.hk/books?id=eBSgoAEACAAJ>.
- [18] He He, Sheng Zha, and Haohan Wang. Unlearn dataset bias in natural language inference by fitting the residual. In *Proceedings of the 2nd Workshop on Deep Learning Approaches for Low-Resource NLP (DeepLo 2019)*, pages 132–142, Hong Kong, China, November 2019. Association for Computational Linguistics. doi: 10.18653/v1/D19-6115. URL <https://www.aclweb.org/anthology/D19-6115>.
- [19] Kaiming He, Xiangyu Zhang, Shaoqing Ren, and Jian Sun. Delving deep into rectifiers: Surpassing human-level performance on imagenet classification. In *Proceedings of the IEEE international conference on computer vision*, pages 1026–1034, 2015.
- [20] Kaiming He, Xiangyu Zhang, Shaoqing Ren, and Jian Sun. Deep residual learning for image recognition. In *Proceedings of the IEEE conference on computer vision and pattern recognition*, pages 770–778, 2016.
- [21] Dan Hendrycks, Kevin Zhao, Steven Basart, Jacob Steinhardt, and Dawn Song. Natural adversarial examples. *arXiv preprint arXiv:1907.07174*, 2019.
- [22] Byeongho Heo, Sanghyuk Chun, Seong Joon Oh, Dongyoon Han, Sangdoon Yun, Youngjung Uh, and Jung-Woo Ha. Slowing down the weight norm increase in momentum-based optimizers. *arXiv preprint arXiv:2006.08217*, 2020.
- [23] Divyansh Kaushik and Zachary C Lipton. How much reading does reading comprehension require? a critical investigation of popular benchmarks. In *Proceedings of the 2018 Conference on Empirical Methods in Natural Language Processing*, pages 5010–5015, 2018.
- [24] Meelis Kull, Miquel Perello Nieto, Markus Kängsepp, Telmo Silva Filho, Hao Song, and Peter Flach. Beyond temperature scaling: Obtaining well-calibrated multi-class probabilities with dirichlet calibration. In *Advances in neural information processing systems*, pages 12316–12326, 2019.

- [25] Balaji Lakshminarayanan, Alexander Pritzel, and Charles Blundell. Simple and scalable predictive uncertainty estimation using deep ensembles. In I. Guyon, U. V. Luxburg, S. Bengio, H. Wallach, R. Fergus, S. Vishwanathan, and R. Garnett, editors, *Advances in Neural Information Processing Systems*, volume 30, pages 6402–6413. Curran Associates, Inc., 2017. URL <https://proceedings.neurips.cc/paper/2017/file/9ef2ed4b7fd2c810847ffa5fa85bce38-Paper.pdf>.
- [26] Tianyu Liu, Zheng Xin, Baobao Chang, and Zhifang Sui. Hyponli: Exploring the artificial patterns of hypothesis-only bias in natural language inference. In *Proceedings of The 12th Language Resources and Evaluation Conference*, pages 6852–6860, 2020.
- [27] Rabeeh Karimi Mahabadi, Yonatan Belinkov, and James Henderson. End-to-end bias mitigation by modelling biases in corpora. In *Annual Meeting of the Association for Computational Linguistics*, 2020.
- [28] Tom McCoy, Ellie Pavlick, and Tal Linzen. Right for the wrong reasons: Diagnosing syntactic heuristics in natural language inference. In *Proceedings of the 57th Annual Meeting of the Association for Computational Linguistics*, pages 3428–3448, 2019.
- [29] Sewon Min, Eric Wallace, Sameer Singh, Matt Gardner, Hannaneh Hajishirzi, and Luke Zettlemoyer. Compositional questions do not necessitate multi-hop reasoning. In *Proceedings of the 57th Annual Meeting of the Association for Computational Linguistics*, pages 4249–4257, 2019.
- [30] Yixin Nie, Xiang Zhou, and Mohit Bansal. What can we learn from collective human opinions on natural language inference data? In *Proceedings of the 2020 Conference on Empirical Methods in Natural Language Processing (EMNLP)*, pages 9131–9143, 2020.
- [31] Ellie Pavlick and Tom Kwiatkowski. Inherent disagreements in human textual inferences. *Transactions of the Association for Computational Linguistics*, 7:677–694, 2019.
- [32] Adam Poliak, Jason Naradowsky, Aparajita Haldar, Rachel Rudinger, and Benjamin Van Durme. Hypothesis only baselines in natural language inference. In *Proceedings of the Seventh Joint Conference on Lexical and Computational Semantics*, pages 180–191, 2018.
- [33] Alec Radford, Karthik Narasimhan, Tim Salimans, and Ilya Sutskever. Improving language understanding by generative pre-training. 2018.
- [34] Victor Sanh, Thomas Wolf, Yonatan Belinkov, and Alexander M Rush. Learning from others’ mistakes: Avoiding dataset biases without modeling them. In *International Conference on Learning Representations*, 2021. URL <https://openreview.net/forum?id=Hf3qXoiNkR>.
- [35] Tal Schuster, Darsh Shah, Yun Jie Serene Yeo, Daniel Roberto Filizzola Ortiz, Enrico Santus, and Regina Barzilay. Towards debiasing fact verification models. In *Proceedings of the 2019 Conference on Empirical Methods in Natural Language Processing and the 9th International Joint Conference on Natural Language Processing (EMNLP-IJCNLP)*, pages 3410–3416, 2019.
- [36] Karen Simonyan and Andrew Zisserman. Very deep convolutional networks for large-scale image recognition. In *International Conference on Learning Representations*, 2015.
- [37] James Thorne, Andreas Vlachos, Christos Christodoulopoulos, and Arpit Mittal. Fever: a large-scale dataset for fact extraction and verification. *arXiv preprint arXiv:1803.05355*, 2018.
- [38] Sunil Thulasidasan, Gopinath Chennupati, Jeff A Bilmes, Tanmoy Bhattacharya, and Sarah Michalak. On mixup training: Improved calibration and predictive uncertainty for deep neural networks. In H. Wallach, H. Larochelle, A. Beygelzimer, F. d’Alché-Buc, E. Fox, and R. Garnett, editors, *Advances in Neural Information Processing Systems*, volume 32, pages 13888–13899. Curran Associates, Inc., 2019. URL <https://proceedings.neurips.cc/paper/2019/file/36ad8b5f42db492827016448975cc22d-Paper.pdf>.
- [39] A. Torralba and A. A. Efros. Unbiased look at dataset bias. In *CVPR 2011*, pages 1521–1528, 2011. doi: 10.1109/CVPR.2011.5995347.

- [40] Prasetya Ajie Utama, Nafise Sadat Moosavi, and Iryna Gurevych. Mind the trade-off: Debiasing nlu models without degrading the in-distribution performance. *arXiv preprint arXiv:2005.00315*, 2020.
- [41] Prasetya Ajie Utama, Nafise Sadat Moosavi, and Iryna Gurevych. Towards debiasing nlu models from unknown biases. In *Proceedings of the 2020 Conference on Empirical Methods in Natural Language Processing (EMNLP)*, pages 7597–7610, 2020.
- [42] Juozas Vaicenavicius, David Widmann, Carl Andersson, Fredrik Lindsten, Jacob Roll, and Thomas Schön. Evaluating model calibration in classification. In Kamalika Chaudhuri and Masashi Sugiyama, editors, *Proceedings of Machine Learning Research*, volume 89 of *Proceedings of Machine Learning Research*, pages 3459–3467. PMLR, 16–18 Apr 2019. URL <http://proceedings.mlr.press/v89/vaicenavicius19a.html>.
- [43] Adina Williams, Nikita Nangia, and Samuel Bowman. A broad-coverage challenge corpus for sentence understanding through inference. In *Proceedings of the 2018 Conference of the North American Chapter of the Association for Computational Linguistics: Human Language Technologies, Volume 1 (Long Papers)*, pages 1112–1122, 2018.
- [44] Rowan Zellers, Ari Holtzman, Yonatan Bisk, Ali Farhadi, and Yejin Choi. Hellaswag: Can a machine really finish your sentence? In *Proceedings of the 57th Annual Meeting of the Association for Computational Linguistics*, pages 4791–4800, 2019.
- [45] Guanhua Zhang, Bing Bai, Jian Liang, Kun Bai, Shiyu Chang, Mo Yu, Conghui Zhu, and Tiejun Zhao. Selection bias explorations and debias methods for natural language sentence matching datasets. In *Proceedings of the 57th Annual Meeting of the Association for Computational Linguistics*, pages 4418–4429, 2019.
- [46] Yuan Zhang, Jason Baldridge, and Luheng He. Paws: Paraphrase adversaries from word scrambling. In *Proceedings of the 2019 Conference of the North American Chapter of the Association for Computational Linguistics: Human Language Technologies, Volume 1 (Long and Short Papers)*, pages 1298–1308, 2019.

## A Experiment Settings

### A.1 Experimental Settings on FEVER

**Bias-only Model** The bias-only model is a nonlinear classifier trained on top of the vector representation of the claim sentence. We obtain this vector representation by max-pooling word embeddings into a single vector as in Utama et al. [40].

**Training Details** We follow Schuster et al. [35] to fine-tune the `bert-base-uncased` model using the following configuration: learning rate is set to  $2 \times 10^{-5}$  and training for 3 epochs. Early stopping on validation accuracy is adopted. We use 5-fold internal cross-validation to train the Dirichlet calibrator and ensemble these calibrators by averaging their predictions. For the Dirichlet calibrator, we drop the bias term, and consider  $\lambda \in \{0.03, 0.06, 0.003, 0.006\}$  and set  $\lambda = 0.06$  in all experiments, according to the in-distribution performance on the development sets. We use 5-fold internal cross-validation to train the Dirichlet calibrator and ensemble these calibrators by averaging their predictions.

### A.2 Experimental Settings on MNLI

**Bias-only Model** For syntactic bias, we train a nonlinear classifier on top of the hand-crafted features. Following Clark et al. [10], the hand-crafted features include (1) whether all words in the hypothesis exist in the premise; (2) whether the hypothesis is a continuous subsequence of the premise; (3) the fraction of premise words that shared with hypotheses; (4) the mean, min, max of cosine similarities between word vectors in the premise and the hypothesis. We consider the same weight for neutral and contradiction class during training by mapping these labels into non-entailment and divide the outputs of non-entailment during debiasing training. For hypothesis-only bias, we train a nonlinear classifier on top of an LSTM-based sentence encoder, which only uses hypothesis sentence as input to predict the labels, as in Utama et al. [40]. For unknown bias, we build a ‘shallow’ model as the bias-only model. It is a `bert-base-uncased` model fine-tuned on a subset of MNLI training set for 3 epochs using the learning rate of  $5 \times 10^{-5}$ . The subset contained 2K examples randomly sampled from MNLI training set, as in Utama et al. [41].

**Training Details** For both hypothesis-only bias and syntactic bias, we fine-tune the `bert-base-uncased` model for all settings using the default configuration: learning rate is set to  $5 \times 10^{-5}$  and training for 3 epochs, as in Utama et al. [40]. The exception is for DRiFt on syntactic bias since we found it convergences slow on the in-distribution development set. We train it for 6 epochs for all settings. Early stopping on validation accuracy is adopted. For unknown bias, we following Utama et al. [41] to fine-tune `bert-base-uncased` model for all settings using the following configuration: learning rate is set to  $5 \times 10^{-5}$  and training for 5 epochs. We observed that MoCaD framework converges faster on the challenging dataset than the original EBD methods. Since the assumption is not having access to any out-of-domain test data, and there is no available development set for HANS, we follow [4; 27] to perform the model section on the test set. Here, we simply pick the model trained at the second-to-last epoch for MoCaD on unknown bias. For the Dirichlet calibrator, we use the same configuration as in FEVER.

## B Proof for Decomposition

*Proof.* In Zhang et al. [45], it is assumed that there exists a *leakage-neutral* distribution  $\mathcal{D}$  with domain  $\mathcal{X} \times \mathcal{Y} \times \mathcal{L} \times \mathcal{S}$ , where  $\mathcal{X}$  is the input feature space,  $\mathcal{L}$  is the sampling strategy feature space and  $\mathcal{S}$  is the binary sampling intention space. The observed distribution is denoted as  $\hat{\mathcal{D}}$ , which satisfies  $\mathbb{P}_{\hat{\mathcal{D}}}(x, y, l) = \mathbb{P}_{\mathcal{D}}(x, y, l | S = Y)$ . In the following, we omit the subscripts for  $\mathcal{D}$ . The following assumptions are adopted in [45]:

$$\mathbb{P}(Y|L) = \mathbb{P}(Y), \tag{6}$$

$$\mathbb{P}(S|X, Y, L) = \mathbb{P}(S|L) \tag{7}$$

In this framework,  $\mathbb{P}(Y|X)$  is supposed to be the true principle to learn, corresponding to  $\mathbb{P}_{\mathcal{D}}(Y|X^S)$  in our notation. Now we prove the following decomposition

$$\mathbb{P}_{\hat{\mathcal{D}}}(Y|X) \propto \mathbb{P}_{\hat{\mathcal{D}}}(Y|L)\mathbb{P}(Y|X)\frac{1}{\mathbb{P}_{\hat{\mathcal{D}}}(Y)} \quad (8)$$

Correspondingly, by our notations we have

$$\mathbb{P}_{\hat{\mathcal{D}}} = \mathbb{P}_{\mathcal{D}}, L = X^B.$$

As a result, equation 8 is equivalent to the decomposition (1) in the main paper. To prove this equation, firstly,

$$\begin{aligned} \mathbb{P}_{\hat{\mathcal{D}}}(Y = y|X) &= \mathbb{P}(Y = y|X, S = Y) \\ &= \frac{\mathbb{P}(Y = y, S = y, X)}{\mathbb{P}(X, S = Y)} \\ &= \frac{\mathbb{P}(S = y|Y = y, L, X^S)\mathbb{P}(Y = y, X)}{\mathbb{P}(X, S = Y)} \\ &= \mathbb{P}(S = y|L)\mathbb{P}(Y = y|X)\frac{\mathbb{P}(X)}{\mathbb{P}(X, S = Y)} \\ &\propto \mathbb{P}(S = y|L)\mathbb{P}(Y = y|X) \end{aligned}$$

Secondly,

$$\begin{aligned} \mathbb{P}_{\hat{\mathcal{D}}}(Y = y|L) &= \mathbb{P}(Y = y|L, S = Y) \\ &= \frac{\mathbb{P}(Y = y, S = y, L)}{\mathbb{P}(L, S = Y)} \\ &= \frac{\mathbb{P}(S = y|Y = y, L)\mathbb{P}(Y = y, L)}{\mathbb{P}(L, S = Y)} \\ &= \mathbb{P}(S = y|L)\mathbb{P}(Y = y)\frac{\mathbb{P}(L)}{\mathbb{P}(L, S = Y)} \end{aligned}$$

By the above equations we have

$$\begin{aligned} \mathbb{P}_{\hat{\mathcal{D}}}(Y = y|X) &\propto \frac{\mathbb{P}_{\hat{\mathcal{D}}}(Y = y|L)}{\mathbb{P}(Y = y)}\mathbb{P}(Y|X)\frac{\mathbb{P}(L, S = Y)}{\mathbb{P}(L)} \\ &\propto \mathbb{P}_{\hat{\mathcal{D}}}(Y = y|L)\mathbb{P}(Y|X)\frac{1}{\mathbb{P}(Y = y)} \end{aligned}$$

As  $\mathbb{P}(Y)$  is a prior parameter chosen to balance the posterior distribution, it can be proved that this condition is satisfied when it equals  $\mathbb{P}_{\mathcal{D}}(Y)$ , as follows:

$$\mathbb{P}_w(Y) \propto \sum_l \frac{\mathbb{P}(Y)}{\mathbb{P}_{\hat{\mathcal{D}}}(Y|L = l)}\mathbb{P}_{\hat{\mathcal{D}}}(Y|L = l)\mathbb{P}_{\hat{\mathcal{D}}}(L = l) = \mathbb{P}(Y)$$

where  $\mathbb{P}_w(Y)$  denotes the distribution of  $Y$  after the reweighting. As a result  $\mathbb{P}_w(Y = y) \propto \mathbb{P}_{\mathcal{D}}(Y = y)$  is satisfied when  $\mathbb{P}(Y = y) = \mathbb{P}_{\mathcal{D}}(Y = y)$ . That ends our proof.  $\square$

## C Useful Notations

We introduce some notations used in the proof of theorems.

**Notations** (Level sets).

$$\begin{aligned} \mathcal{S}_B(b) &:= \{x \in \mathcal{X} | \mathbb{P}_{\mathcal{D}}(Y = 0 | X^B = x^b) = b\} \\ \mathcal{S}_{f_B}(l) &:= \{x \in \mathcal{X} | p_0^b(X = x) = l\}. \\ \mathcal{S}_E(a) &:= \{x \in \mathcal{X} | \mathbb{P}_{\mathcal{D}}(Y = 0 | X = x) = a\} \\ \mathcal{S}_R(s) &:= \{x \in \mathcal{X} | \mathbb{P}(Y = 0 | X^S = x^s) = s\} \end{aligned}$$

**Notation** ( $\tilde{s}$ ).

$$\tilde{s}_{a,b} = \frac{a(1-b)}{a(1-b) + b(1-a)}$$

**Notations** ( $Y^S, \tilde{Y}, \hat{Y}$ ).

$$Y^S(x) := \operatorname{argmax}_{i \in \mathcal{Y}} \mathbb{P}_{\mathcal{D}}(Y = i | X^S = x^s), \quad (9)$$

$$\tilde{Y}(x) := \operatorname{argmax}_{i \in \mathcal{Y}} \mathbb{P}_{\mathcal{D}, f_M^*}(Y = i | X = x). \quad (10)$$

$$\hat{Y}(x) := \operatorname{argmax}_{i \in \mathcal{Y}} \mathbb{P}_{\mathcal{D}}(Y = i | X = x) \quad (11)$$

**Notation** ( $\mathcal{P}^i(\cdot)$ ). Denote  $\mathcal{P}^i(\mathcal{S}) := \mathbb{P}_{\mathcal{D}}(Y^S = i | \mathcal{S})$ .

**Definition 1** (False Reversal Rate). *For an input  $x$ , we say  $f_B(x)$  induces a false reversal if  $\tilde{Y}(x) \neq \hat{Y}(x) = Y^S(x)$ . The false reversal rate of a set  $\mathcal{S}$  is defined as  $\frac{\mathbb{P}_{\mathcal{D}}(\mathcal{S}_{fr})}{\mathbb{P}_{\mathcal{D}}(\mathcal{S})}$ , where  $x \in \mathcal{S}_{fr}$  if it occurs false reversal and  $x \in \mathcal{S}$ .*

Similarly we define the False Agreement Rate:

**Definition 2** (False Agreement Rate). *For an input  $x$ , we say  $f_B(x)$  induces a false agreement, if  $\tilde{Y}(x) = \hat{Y}(x) \neq Y^S(x)$ . The false agreement rate of a set  $\mathcal{S}$  is defined as  $\frac{\mathbb{P}_{\mathcal{D}}(\mathcal{S}_{fa})}{\mathbb{P}_{\mathcal{D}}(\mathcal{S})}$ , where  $x \in \mathcal{S}_{fa}$  if it occurs false agreement and  $x \in \mathcal{S}$ .*

## D Proof of Theorem 1

First we prove the following lemma.

**Lemma 3.** *Denote  $\mathcal{R}_b(a) := \mathcal{P}^1(\mathcal{S}_E(a) \cap \mathcal{S}_B(b))$ , and  $p_B(a|b) := \mathbb{P}_{\mathcal{D}}(\mathcal{S}_E(a) | \mathcal{S}_B(b))$ . We have*

$$\mathcal{R}_b(a) = \mathcal{P}^1(\mathcal{S}_R(\tilde{s}_{a,b})) = I(\tilde{s}_{a,b} < 0.5), \quad (12)$$

$$p_B(a|b) = C_{a,b} \mathbb{P}_{\mathcal{D}}(\mathcal{S}_R(\tilde{s}_{a,b})), \quad (13)$$

where  $C_{a,b} = \frac{1}{2}(\frac{a}{b} + \frac{1-a}{1-b})^{-1}$ .

*Proof.* For the first equation, it is obvious that  $\mathcal{S}_E(a) \cap \mathcal{S}_B(b) = \mathcal{S}_R(\tilde{s}_{a,b}) \cap \mathcal{S}_B(b)$ . Then we have

$$\mathcal{P}^1(\mathcal{S}_E(a) \cap \mathcal{S}_B(b)) = \mathcal{P}^1(\mathcal{S}_R(\tilde{s}_{a,b}) \cap \mathcal{S}_B(b)).$$

By the definition of  $\mathcal{P}^1$  we have

$$\mathcal{P}^1(\mathcal{S}_R(\tilde{s}_{a,b}) \cap \mathcal{S}_B(b)) = \mathcal{P}^1(\mathcal{S}_R(\tilde{s}_{a,b})) = I(\tilde{s}_{a,b} < 0.5)$$

The first equation follows.

By  $X^S \perp\!\!\!\perp X^B | Y$  on  $\mathbb{P}_{\mathcal{D}}$ , As  $\mathbb{P}(Y = 0 | X^S)$  is a function of  $X^S$ ,  $\mathbb{P}_{\mathcal{D}}(Y = 0 | X^B)$  is a function of  $X^B$ , we have

$$\mathbb{P}_{\mathcal{D}}(Y = 0 | X^S) \perp\!\!\!\perp \mathbb{P}_{\mathcal{D}}(Y = 0 | X^B) | Y \quad (14)$$

Without loss of generality, we can assume that  $\mathbb{P}_{\mathcal{D}}(Y = 0 | X^S)$  takes value in a discrete set  $\mathcal{V}$ . By the decomposition that

$$\mathbb{P}_{\mathcal{D}}(Y | X) \propto \mathbb{P}_{\mathcal{D}}(Y | X^B) \mathbb{P}_{\mathcal{D}}(Y | X^S)$$

We have

$$\begin{aligned} \mathbb{P}_{\mathcal{D}}(\mathcal{S}_E(a) | \mathcal{S}_B(b)) &= \sum_{i=0,1} \mathbb{P}_{\mathcal{D}}(\mathcal{S}_R(\tilde{s}_{a,b}) | \mathcal{S}_B(b), Y = i) \mathbb{P}_{\mathcal{D}}(Y = i | \mathcal{S}_B(b)) \\ &= \sum_{i=0,1} \mathbb{P}_{\mathcal{D}}(\mathcal{S}_R(\tilde{s}_{a,b}) | Y = i) \mathbb{P}_{\mathcal{D}}(Y = i | \mathcal{S}_B(b)) \\ &= \sum_{i=0,1} \frac{1}{2} \mathbb{P}_{\mathcal{D}}(Y = i | \mathcal{S}_R(\tilde{s}_{a,b})) \mathbb{P}_{\mathcal{D}}(\mathcal{S}_R(\tilde{s}_{a,b})) \mathbb{P}_{\mathcal{D}}(Y = i | \mathcal{S}_B(b)) \\ &= \frac{1}{2} (\tilde{s}_{a,b} \cdot b + (1 - \tilde{s}_{a,b})(1 - b)) \mathbb{P}_{\mathcal{D}}(\mathcal{S}_R(\tilde{s}_{a,b})) \\ &= \frac{1}{2} \left( \frac{a}{b} + \frac{1-a}{1-b} \right)^{-1} \mathbb{P}_{\mathcal{D}}(\mathcal{S}_R(\tilde{s}_{a,b})). \end{aligned}$$

The second equation follows.  $\square$



Now we start the proof of the theorem.

*Proof.* Without the loss of generality, consider the case when  $l_0 > 0.5$ . The proof for  $l_0 < 0.5$  has a symmetric form. Denote  $\mathcal{R}(a) := \mathcal{P}^1(\mathcal{S}_E(a) \cap \mathcal{S}_{f_B}(l))$ , and  $p_f(a|l) := \mathbb{P}_{\mathcal{D}}(\mathcal{S}_E(a)|\mathcal{S}_{f_B}(l))$ . The False Reversal Rate and False Agreement Rate on  $\mathcal{S}_{f_B}(l)$  is

$$\mathcal{FR}(l) = \sum_a \mathcal{R}(a)p_f(a|l)I(a > l)I(a < 0.5) + (1 - \mathcal{R}(a))p_f(a|l)I(a < l)I(a > 0.5) \quad (15)$$

$$\mathcal{FA}(l) = \sum_a (1 - \mathcal{R}(a))p_f(a|l)I(a < l)I(a < 0.5) + \mathcal{R}(a)p_f(a|l)I(a > l)I(a > 0.5) \quad (16)$$

The total debiasing error on  $\mathcal{S}_{f_B}(l)$  is the summation of False Reversal Rate and False Agreement Rate, which denoted as  $E(l)$ . The difference of total debiasing error at  $l = a$  is

$$\Delta E(a) = (1 - 2\mathcal{R}(a))p_f(a|l) \quad (17)$$

$\Delta E(a) < 0$  when  $\mathcal{R}(a) \in [0, 0.5)$ ,  $p_f(a|l) > 0$ ,  $\Delta E(a) > 0$  when  $\mathcal{R}(a) \in (0.5, 1]$ ,  $p_f(a|l) < 0$ . By that, when  $p_f(a|l) > 0, \forall a \in (0, 1)$ , the total debiasing error is minimized at  $a$  s.t.  $\mathcal{R}(a) = 0.5$ .

Denote  $p_f^B(b|l) := \mathbb{P}_{\mathcal{D}}(\mathcal{S}_B(b)|\mathcal{S}_{f_B}(l))$ . We have

$$\mathcal{R}(a) = \sum_b \mathcal{R}_b(a)p_B(a|b)p_f^B(b|l) \frac{1}{p_f(a|l)} \quad (18)$$

We suppose the support of  $\mathbb{P}_{\mathcal{D}}(Y = 0|X^B)$  condition on  $\mathcal{S}_{f_B}(l)$  is on  $(l_0 - \epsilon, l_0 + \epsilon)$ , i.e.  $p_f^B(b|l)$  is non-zero only if  $b \in (l_0 - \epsilon, l_0 + \epsilon)$ .

By Lemma 3, we have

$$\mathcal{R}_b(a) = I(\tilde{s}_{a,b} < 0.5) \quad (19)$$

When  $a \in (l_0 + \epsilon, 1)$ ,  $\tilde{s}_{a,b} > 0.5, \forall b$ . Thus  $\mathcal{R}_b(a) = 1, \forall b$ . We have

$$\mathcal{R}(a) = \sum_b p_B(a|b)p_f^B(b|l) \frac{1}{p_f(a|l)} = 1 \quad (20)$$

Similarly it can be derived that  $\mathcal{R}(a) = 0$  when  $a \in (0, l_0 - \epsilon)$ . As a result, the debiasing error is non-decreasing as  $l$  decreases on the interval  $(0, l_0 - \epsilon)$  or increases on the interval  $(l_0 + \epsilon, 1)$ , i.e. The debiasing error increases as  $|l - \mathbb{P}_{\mathcal{D}}(Y = 0|\mathcal{S}_{f_B}(l))|$  increases. Denote the absolute difference between  $\mathbb{P}_{\mathcal{D}}(Y = 0|\mathcal{S}_{f_B}(l))$  and  $l_{opt}$  which minimizes the debiasing error  $E$  as  $\delta(l_0, \epsilon, \alpha)$ . As

$$\mathbb{P}_{\mathcal{D}}(Y = 0|\mathcal{S}_{f_B}(l)) = \sum_b b p_f^B(b|l) \in (l_0 - \epsilon, l_0 + \epsilon), \quad (21)$$

$l_{opt} \in (l_0 - \epsilon, l_0 + \epsilon)$ , we have  $\delta(l_0, \epsilon, \alpha) < 2\epsilon$ .

Now we consider the case when  $\alpha := \min_{X^S} \max_{i \in \{0,1\}} \mathbb{P}_{\mathcal{D}}(Y = i|X^S) > 0$ , i.e.  $\mathbb{P}_{\mathcal{D}}(\mathcal{S}_R(s)) = 0$  when  $s \in (1 - \alpha, \alpha)$ . When  $\tilde{s}_{a,b} \in (1 - \alpha, \alpha)$ , by Lemma 1  $p_B(a|b) = 0$ , and we have

$$a \in \left( \frac{b}{\frac{1-b}{1-\alpha} + 2b - 1}, \frac{b}{\frac{1-b}{\alpha} + 2b - 1} \right) =: (L_{\alpha,b}, U_{\alpha,b}) \quad (22)$$

Both  $L_{\alpha,b}$  and  $U_{\alpha,b}$  increase as  $b$  increase. As a result, for  $\forall a \in (L_{\alpha,l_0+\epsilon}, U_{\alpha,l_0-\epsilon})$ ,  $p_f(a|l) = \sum_b p_B(a|b)p_f^B(b|l) = 0$ . When  $l_0 - \epsilon = L_{\alpha,l_0+\epsilon}$ , we have

$$\alpha = \frac{1}{2} + \frac{\epsilon}{2l_0(1-l_0) + 2\epsilon^2} =: C_{\alpha} \quad (23)$$

When  $l_0 + \epsilon = U_{\alpha,l_0-\epsilon}$ , we also have  $\alpha = C_{\alpha}$ . As  $L_{\alpha,l_0+\epsilon}$  decreases and  $U_{\alpha,l_0-\epsilon}$  increases with  $\alpha$ , when  $\alpha < C_{\alpha}$ , we have the same conclusion:  $\Delta E(a) \geq 0$  when  $a \in (l_0 + \epsilon, 1)$  and  $\Delta E(a) \leq 0$  when  $a \in (0, l_0 - \epsilon)$ , and  $\delta(l_0, \epsilon, \alpha) < 2\epsilon$ . That gives the first conclusion in Theorem 1.

For the case when  $\alpha > C_\alpha$ ,  $L_{\alpha, l_0 + \epsilon} < l_0 - \epsilon$  and  $U_{\alpha, l_0 - \epsilon} > l_0 + \epsilon$ . We consider the quantity  $l_0 - \epsilon - L_{\alpha, l_0 + \epsilon}$  and  $U_{\alpha, l_0 - \epsilon} - l_0 + \epsilon$ . Denote  $D(\alpha, l_0, \epsilon) = 2l_0 - (L_{\alpha, l_0 + \epsilon} + U_{\alpha, l_0 - \epsilon})$ . We have

$$\frac{\partial D}{\partial \alpha} = \frac{(l_0 + \epsilon)(1 - l_0 - \epsilon)}{(1 - (l_0 + \epsilon) + 2(l_0 + \epsilon - 1)(1 - \alpha))^2} - \frac{(l_0 - \epsilon)(1 - l_0 + \epsilon)}{(1 - (l_0 - \epsilon) + 2(l_0 - \epsilon - 1)\alpha)^2} \quad (24)$$

$$= \frac{-(2l_0 - 1)[2\epsilon\alpha^2 + 2\alpha(l_0 + \epsilon)(l_0 - \epsilon) - 2\alpha(l_0 + \epsilon) - (l_0 + \epsilon)(l_0 - \epsilon) + l_0 + \epsilon]}{(1 - (l_0 + \epsilon) + 2(l_0 + \epsilon - 1)(1 - \alpha))^2(1 - (l_0 - \epsilon) + 2(l_0 - \epsilon - 1)\alpha)^2} \quad (25)$$

$$=: -\frac{1}{A}[2\epsilon\alpha^2 + 2\alpha(l_0 + \epsilon)(l_0 - \epsilon) - 2\alpha(l_0 + \epsilon) - (l_0 + \epsilon)(l_0 - \epsilon) + l_0 + \epsilon], A > 0 \quad (26)$$

There exists  $\alpha'$  s.t.  $\frac{\partial D}{\partial \alpha}(\alpha, l_0, \epsilon) < 0$  when  $\alpha < \alpha'$ ,  $\frac{\partial D}{\partial \alpha}(\alpha, l_0, \epsilon) > 0$  when  $\alpha > \alpha'$ . When  $\alpha = C_\alpha$ ,

$$\frac{\partial D}{\partial \alpha}(C_\alpha, l_0, \epsilon) = \frac{2\epsilon(l_0 + \epsilon)(l_0 - \epsilon)(1 - (l_0 + \epsilon))(1 - (l_0 - \epsilon))}{A[2(l_0 + \epsilon)(l_0 - \epsilon) - 2l_0]^2} > 0 \quad (27)$$

Thus  $D(\alpha, l_0, \epsilon) > D(C_\alpha, l_0, \epsilon) = 0$  when  $\alpha > C_\alpha$ . Denote  $C := l_0 - \epsilon - \frac{l_0 + \epsilon}{(l_0 + \epsilon) + (1 - l_0 - \epsilon)\frac{\alpha}{1 - \alpha}}$ , we have  $l_{opt} \in (l_0 - \epsilon - C, U_{\alpha, l_0 - \epsilon})$ , as a result  $C < \delta(l_0, \epsilon, \alpha) < 2\epsilon + C$ . That ends our proof.  $\square$

## E Proof of Theorem 2

*Proof.* As  $\tilde{Y}(X) = 0$  if and only if  $\mathbb{P}_{f_B}(Y = 0|X) > \mathbb{P}_{f_B}(Y = 1|X)$ . The later is equivalent to

$$\mathbb{P}_{\mathcal{D}}(Y = 0|X)/q_0^b(x) > \mathbb{P}_{\mathcal{D}}(Y = 1|X)/q_1^b(x),$$

equivalently

$$\mathbb{P}_{\mathcal{D}}(Y = 0|X) > q_0^b(x).$$

As a result, when  $\hat{Y}(X) \neq \tilde{Y}(X)$ , we have

$$\mathbb{P}_{\mathcal{D}}(Y = \hat{Y}(x)|X = x) < q_{\hat{Y}(x)}^b(x)$$

Conversely, the above equation induces  $\tilde{Y}(X) \neq \hat{Y}(X)$ .  $\square$

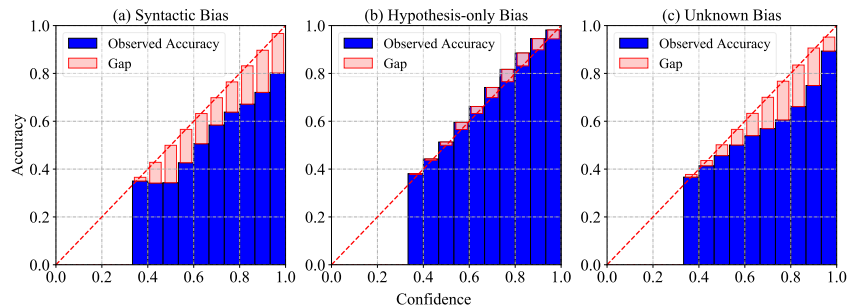


Figure 4: Reliability diagrams of the bias-only models on MNL. On MNL, (a) the syntactic bias-only model and (c) the unknown bias-only model are over-confident, (b) the hypothesis-only bias-only model is under-confident.

## F Over- or Under-Confidence of the Bias-only Model on MNL

We plot the confidence-reliability diagram [15] of these three models in Figure 4. The wide blue bars show the average accuracy of the bias-only model, and the narrow red bars show the gap between the average accuracy and the confidence of the bias-only model, i.e., the uncertainty estimation on the predicted class. For perfectly calibrated predictions, the curve in a reliability diagram should be as close as possible to the diagonal. Most of the blue bars below the diagonal indicate that the model is over-confident, otherwise is under-confident. It can be observed that the syntactic bias-only model and unknown bias-only model are over-confident, and the hypothesis-only bias-only model is under-confident.

## G The Classification Accuracy of the Calibrated Bias-only Models

To facilitate the study, we demonstrate the classification accuracy of the calibrated bias-only models on different training datasets, as shown in Table 4. In the table, Un-Cal, Dirichlet, and TempS denote the bias-only model without calibration, with temperature scaling and Dirichlet calibrator, respectively.

Table 4: Accuracy of the calibrated bias-only models on different training datasets.

	FEVER	HANS	MNL	Unknown
Un-Cal	60.6	54.8	63.8	63.2
TempS	60.6	54.8	63.8	63.2
Dirichlet	62.7	69.9	64.0	63.4

## H Experiment on Image Classification

In image classification experiments, we validate the effectiveness of MoCaD on the texture bias in realistic images.

**Datasets** We follow Bahng et al. [2] to conduct our experiment. The experiment is conducted on the 9-Class Imagenet dataset [2], which is a subset of ImageNet [12] containing 9 super-classes. The validation dataset and ImageNet-A [21] are used for evaluation. For the in-distribution validation dataset, an ‘unbiased’ accuracy measurement is used to evaluate the debiasing performance, denoted as *Unbiased*. It first obtains the proxy ground truths  $c \in \{1, \dots, K\}$  for texture bias using texture feature clustering. Then the dataset is grouped according to the texture-class combination  $(c, y)$ . The combination-wise accuracy  $A_{c,y}$  is computed by  $\text{Corr}(c, y) / \text{Pop}(c, y)$ , where  $\text{Corr}(c, y)$  is the number of correctly predicted samples in  $(c, y)$  and  $\text{Pop}(c, y)$  is the total number of samples in

$(c, y)$ . Finally, `Unbiased` is the mean accuracy over all  $A_{c,y}$  where the population  $\text{Pop}(c, y) > 10$ . Specifically, the texture features are extracted from images by computing the gram matrices of low-layer feature maps to capture the edge and color cues. It uses the feature maps from layer `relu1_2` of the ImageNet pre-trained VGG16 [36]. The clustering process is done with the mini-batch k-means algorithm with  $k = 9$  and batch size 1024. As k-means clustering is non-convex, the clustering is repeated three times with different initialization, and the averaged performance across the three trials is reported. ImageNet-A [21] is a dataset of natural adversarial filtered images that fool ImageNet-trained ResNet50 [20]. The images consist of many failure modes of networks when “frequently appearing background elements” [21] become erroneous cues for recognition.

**Main Model and Bias-only Model** Following [2], the main model is a fully convolutional network followed by a global average pooling (GAP) layer and a linear classifier. Specifically, ResNet-50 architecture [20] is adopted as the main model. The bias-only model is a CNN with smaller receptive fields, which is expected to be biased towards texture bias. Specifically, it is a `BagNet` [6], which is a variant of the ResNet50 architecture, by replacing many  $3 \times 3$  with  $1 \times 1$  convolutions, thereby limiting the receptive field size of the topmost convolutional layer.

Table 5: Classification accuracy on image classification.

Method	ID	UnBiased	ImageNet-A
PoE	94.6 $\pm$ 0.2	94.3 $\pm$ 0.3	31.8 $\pm$ 1.9
<b>PoE</b> <sub>TempS</sub>	94.7 $\pm$ 0.3	<b>94.5</b> $\pm$ 0.3	<b>31.9</b> $\pm$ 1.1
<b>PoE</b> <sub>Dirichlet</sub>	94.6 $\pm$ 0.4	94.3 $\pm$ 0.4	30.5 $\pm$ 1.2
DRiFt	94.6 $\pm$ 0.2	94.4 $\pm$ 0.3	31.9 $\pm$ 0.8
<b>DRiFt</b> <sub>TempS</sub>	94.8 $\pm$ 0.4	<b>94.4</b> $\pm$ 0.4	<b>32.5</b> $\pm$ 1.2
<b>DRiFt</b> <sub>Dirichlet</sub>	94.5 $\pm$ 0.2	94.3 $\pm$ 0.2	32.4 $\pm$ 1.0
InvR	94.5 $\pm$ 0.4	94.1 $\pm$ 0.5	31.6 $\pm$ 0.3
<b>InvR</b> <sub>TempS</sub>	94.3 $\pm$ 0.1	93.8 $\pm$ 0.1	<b>32.2</b> $\pm$ 1.5
<b>InvR</b> <sub>Dirichlet</sub>	94.4 $\pm$ 0.4	<b>94.2</b> $\pm$ 0.2	31.8 $\pm$ 0.9
LMin	90.9 $\pm$ 0.5	90.5 $\pm$ 0.6	27.7 $\pm$ 1.6
<b>LMin</b> <sub>TempS</sub>	91.1 $\pm$ 0.6	90.6 $\pm$ 0.6	<b>28.1</b> $\pm$ 1.8
<b>LMin</b> <sub>Dirichlet</sub>	91.2 $\pm$ 0.2	<b>90.9</b> $\pm$ 0.2	26.1 $\pm$ 0.8

**Training Details and Configurations** We follow the configuration in [2]: the batch size is set to 128; learning rates are initially set to 0.001 and are decayed by cosine annealing and training for 120 epochs. As advised by Bahng et al. [2], we use AdamP optimizer [22] in the experiment. We experiment with 8 implementations of MoCaD, i.e. two different calibrators combined with four different ensembling strategies as the same as in previous experiments. For Learned-Mixin, the entropy term weight is set to the value suggested by [2]. We run each experiment five times and report the mean scores and the standard deviations. For the Dirichlet calibrator, we use the same configuration as in FEVER.

**Experimental Results** Table 5 shows the experimental result on image classification. We can see that our MoCaD can achieve the best debiasing performance among all EBD methods, but the improvement is inconsistent. According to our theoretical analysis, that may be because the invariant mechanism for image classification task has a higher certainty (bigger  $\alpha$ ), reducing the impact of calibration error on debiasing.